Map Building with Radar and Motion Sensors for Automated Highway Vehicle Navigation

Katsumi Kimoto*
Department of Information Science
Kyoto University
Yoshidahonmachi Sakyoku
Kyoto 606-01, JAPAN
kimoto@kuis.kyoto-u.ac.jp

Chuck Thorpe
The Robotics Institute
Carnegie Mellon University
5000 Forbes Avenue
Pittsburgh Pennsylvania 15213, U.S.A
cet@cs.cmu.edu

Abstract

Driving autonomous vehicles on the highway is one of the most important coming applications of autonomous mobile robots.

Many vision based systems have been developed for highway navigation and their success in experiments have been reported. While they have impressive success, they cannot as yet handle all conditions of weather, illumination, and traffic. Thus it is still necessary to develop other navigation methods to enable redundant and robust navigation systems.

In contrast to road-following applications, off-road navigation usually cannot rely on simple tracking of visual cues, and therefore must use position-based and landmark-based navigation, such as in [4, 5]. Our long-term goal is to integrate this style of position-based navigation with visual road following in order to build a more robust and reliable road navigation system.

In this paper, we describe the first part of that project: constructing a navigation system that can build maps of highways and landmarks, and use those feature for position-based navigation. Speed and yaw rate gyro sensors are used for vehicle motion detection, and a millimeter wave radar system is used for landmark detection. To achieve position estimation and error correction, we use an extended Kalman filter.

First, a map is built without previous knowledge of landmarks while human drives the vehicle. Then, at the stage of autonomous navigation, the previously produced map is used for position estimation. The experimental results show that a map produced by the proposed method can be used for later navigation, and that vehicle position is estimated accurately.

1 Introduction

Many different vision based navigation system have been developed. One of the pioneer was Graefe et.al. in Germany [3]. They developed a real-time vision processing system, and demonstrated highway navigation. In the United States, Pomealau et.al. developed a neural network based navigation system called ALVINN [1]. Later they replaced the system with non-neural network based one called RALPH [2]. These vision systems find the road geometry ahead, and control steering so that the vehicle can follow the highway.

Even though these vision based system succeeded in experimental runs, it is still necessary to develop other navigation method to make redundant and tolerant system. The longest runs without human intervention using the RALPH system, for example, were over 90 miles. This is impressive performance for a research system, but is still not adequate for a production system.

In contrast with highway system, many non highway autonomous vehicles use positioning and landmark system [4, 5] etc., because non highway environment is more complex than highway environment, and position information helps environment recognition by vision or other sensors. In this paper, we describe the first results of our system which uses this kind of landmark based navigation for highway driving. It is our intent in further work to integrate the position-based navigation, reported here, with other ongoing work in vision-based navigation, in order to produce a more robust driving system.

For position based navigation, our system requires an accurate map of environment. This paper first describes methods for building such a map, then discusses techniques for using it.

2 Strategy of Navigation

In a highway environment the path that the vehicle should follow is limited to the constructed roadway. The vehicle must stay in its lane, and changing lanes must be prohibited unless intended. Then free space in which the vehicle can move is very limited.

The problem is not planning or selection of the path,

*This research was achieved when the first author stayed at Carnegie Mellon University from 1995 to 1997.

Proc. IROS 97 0-7803-4119-8/97/$10©1997 IEEE

Table 1: System Parameters and Technical Specifications for the FMCW Radar

Carrier Frequency	76.5 GHz
Modulation Waveform	FMCW
Swept Frequency	300 MHz
Range	
Coverage	1 ~ 200 m
Resolution	1 m
Accuracy	0.1 m (or better)
Azimuth	
Coverage	12°
Resolution	3°
Nominal Accuracy	0.1°
Elevation Coverage	3°
Antenna : 1 Transmitter, 4 Receiver linear array VFoV: 3°, HFoV: 12° for each Antenna	

but rather specification of an accurate path and positioning.

In our system, the path is described in a map, and the map is built while an operator drives on the highway. The location of the vehicle is measured by motion sensors, and landmark observation is recorded simultaneously.

The problem of map building and positioning with motion sensors is that the vehicle position can not be obtained directly from inertia or motion sensors, but it is calculated by integrating sensor data. Errors in sensor data, modeling, and calculation, accumulate in each iteration of calculation, so that the error in calculated vehicle position could be unacceptable when the vehicle moves a long distance. This error must be corrected by observation of landmarks. To achieve this position estimation and error correction the extended Kalman filter (EKF) is used.

3 Radar and Motion Sensors

3.1 Radar Range Finder

A millimeter wave radar system for outdoor vehicle navigation has been developed in our group at Carnegie Mellon University [6]. The radar system operates as a Frequency Modulated Continuous Wave (FMCW) system. The system parameters and specification are shown in Table 1.

The radar system provides two dimensional position information (range and bearing) of objects. The amplitude of the reflected wave from each object is also obtained. The detectable range is up to 200 meters and the maximum bearing angle is ±6 degrees.

The radar is used to detect landmarks beside the roadway. Landmarks may be corner cubes specially installed for vehicle navigation or natural metallic objects such as traffic signs and light poles.

3.2 Doppler Effect Compensation

In the process of radar sensing the Doppler effect cannot be ignored [6]. The Doppler effect causes a range error of radar sensing which is proportional to the relative speed of the vehicle and objects. This range error can be about 5m when vehicle is running at 100km/h. Accuracy of landmark position is critically important for map building and navigation, so we need to correct for the Doppler shift in the radar output by using motion sensor data. In a typical situation, the radar is moving with vehicle, and we assume the reflection comes from a stationary object in front of the vehicle. The frequency shift f_d in the received wave is

$$f_d = \frac{2v}{\lambda} \tag{1}$$

where λ is the wavelength of the transmitted wave, and v is the relative speed of the vehicle and the object [7].

The range error ΔR caused by the Doppler effect can be calculated as follows [6].

$$\begin{aligned} \Delta R &= \frac{c}{4\Delta f f_m} f_d \\ &= \frac{c}{2\Delta f f_m} \cdot \frac{v}{\lambda} \end{aligned} \tag{2}$$

where the carrier frequency is 76.5GHz, we have a wavelength $\lambda = c/f = 3.9$[mm]. For our system, we have a swept frequency of $2\Delta f = 300$[MHz], a modulation frequency $f_m = 1.25$[kHz] and c is the speed of light. Then the result is

$$\Delta R = 0.204v \quad \text{[m]} \tag{3}$$

When $v = 27$[m/s] which is approximately 100km/h, the range error will be 5.5[m]. We use equation (3) to compensate for the Doppler effect in the range data by using the vehicle velocity v obtained by the speed sensor.

3.3 Motion Sensors

Dimensions. Vehicle motion is measured by a vehicle speed sensor and a yaw rate gyro sensor. The measured motion and position, and thus the constructed map, are only two dimensional, although the actual road may not be exactly planar. Although the constructed map may not be exactly accurate, since it does not represent true 3-D road shape, it is still useful for navigation because later passes over the same terrain with the same sensors will have similar sources of error.

Speed Sensor. The forward component of the vehicle velocity is measured by a commercial non-contact optical speed sensor. The speed sensor detects the

Table 2: The Speed Sensor Specifications

DATRON Corporation model DLS-1

Sensor resolution	2.5mm
Diameter of optical field	30mm
Speed measurement range	0.5Kmh to 400Kmh
Accuracy	±0.2%
Repeatability	±0.1%

Table 3: The Gyro Sensor Specifications

ANDREW Corporation model AUTOGYRO 225140

Description	Specification
Input Rotation Rate	±100deg/sec
Angle Random Walk	
deg/hr/rt-Hz	20
deg/rt-hr	0.33
Bias Drift	
(at fixed temperature)	0.005deg/sec
(repeatability)	0.025deg/sec
Scale Factor Linearity	
constant temp.	< 0.5%
full temp.	< 1%

flow of optical texture of the ground so that the traveled distance is obtained. By counting the distance travelled in a small time interval, the vehicle forward speed is obtained. Table 2 shows the specifications of the speed sensor.

Yaw Rate Gyro Sensor. The other motion sensor is a yaw rate gyro sensor which we use with the speed sensor to provide a complete 2-D motion measurement. The specifications of the gyro sensor is shown in Table 3.

4 Kalman Filter Design for Map Building

4.1 vehicle kinematics

The speed sensor measures the forward component of the vehicle velocity, and the yaw rate gyro sensor measures the angular velocity around the vehicle's vertical axis.

These two sensors are sufficient to measure the two dimensional displacement of the vehicle. We assume the vehicle body, on which the sensor coordinate is fixed, is always standing straight up, because the vehicle does not turn sharply on highways and therefore does not roll or pitch significantly. The advantage of this set of motion sensors is that the filter design can

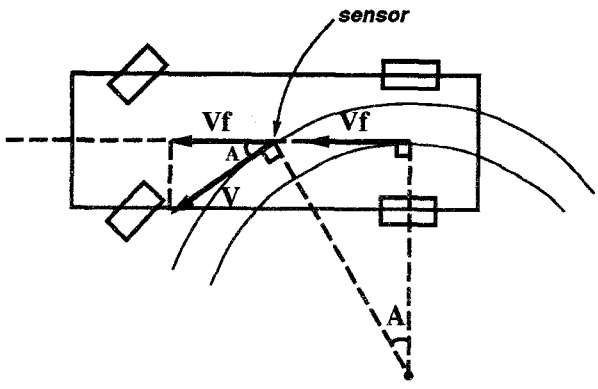

Figure 1: Speed Sensor Configuration

be simpler than systems which use wheel rotation or steering angle for motion detection.

The vehicle kinematics are

$$\begin{aligned} x(t) &= \int_0^t v(t)\cos\theta(t)dt \\ y(t) &= \int_0^t v(t)\sin\theta(t)dt \\ \theta(t) &= \int_0^t \omega(t)dt \end{aligned} \tag{4}$$

where, $(x(t), y(t))$ is the relative position of the vehicle in the two dimensional plane, and $\theta(t)$ is the vehicle orientation described by the angle between vehicle heading and the x-axis. $v(t)$ and $\omega(t)$ are the speed and angular velocity of the vehicle respectively. In discrete form in time, t_k, $k = 1, 2, 3, ...$, equations(4) can be written as follows.

$$\begin{aligned} x_{k+1} &= x_k + v_k \Delta t \cos\theta_k \\ y_{k+1} &= y_k + v_k \Delta t \sin\theta_k \\ \theta_{k+1} &= \theta_k + \omega_k \Delta t \end{aligned} \tag{5}$$

where Δt is the interval between each successive time step.

4.2 Models of Sensor Errors

Speed Sensor. The speed sensor is attached to the vehicle so that the sensor is aligned along the vehicle forward direction.

If the alignment is perfect, the sensor detects the forward component of vehicle velocity correctly. In Figure 1 V is the vehicle velocity at the point where the sensor is attached. V_f is the sensor output, which is the velocity along the direction in which the sensor is pointing. If the sensor is properly aligned with the vehicle, then the forward velocity of the vehicle's coordinate frame (centered between the rear wheels) is also given by V_f.

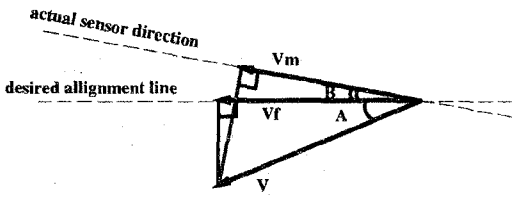

Figure 2: Alignment Error of Speed Sensor

However in practice, the sensor alignment can not be perfect. Any errors in alignment can be exacerbated if the sensor is not mounted on the rear axle and the center line of the vehicle.

We will consider the sensor error caused by this misalignment. Assume that the angle of misalignment from the center line is B as shown in Figure 2 and the sensor output V_m has an error caused by B. Let A be the angle between the vehicle forward direction and the direction of velocity V. V_f and V_m are projections of the vehicle velocity V onto the desired alignment line and the actual sensor direction respectively.

$$\begin{aligned} V_f &= V\cos A \\ V_m &= V\cos(A+B) \end{aligned} \tag{6}$$

Then, we obtain

$$\begin{aligned} V_m &= V_f\frac{\cos(A+B)}{\cos A} \\ &= V_f(1-B\tan A-\frac{1}{2}B^2)+O(B^3) \end{aligned} \tag{7}$$

The angle A varies according to the curvature of the vehicle trajectory, and the angle B is the fixed error of alignment. If the sensor is fixed very close to the vehicle rear axle, $\tan(A) \ll B$, then $|B\tan(A)| \ll \frac{1}{2}B^2$. Note that $\frac{1}{2}B^2$ is an unknown constant value. We model the sensor measurement

$$v_s = V_f(1+p) \tag{8}$$

where v_s is the sensor output. p is a term caused by alignment error.

Gyro Sensor. The yaw rate gyro sensor gives us angular velocity around the vertical axis. We model the gyro sensor output such that the sensor output includes a scale factor error and offset (bias drift) errors. The sensor output ω_s is written as follows.

$$\omega_s = \omega(1+q)+r \tag{9}$$

where q and r are scale factor error and offset error respectively. We assume that both errors change smoothly because the average of those errors depends mainly on temperature.

4.3 Prediction of Vehicle State

Now we can proceed to derive the equations of prediction using the extended Kalman filter technique. In addition to vehicle position and orientation $(x,y,\theta)^T$ we take sensor error parameters $(p,q,r)^T$ as vehicle state $\boldsymbol{x}=(x,y,\theta,p,q,r)$. From equation(4), (8), (9), and input $\hat{\boldsymbol{m}}=(\hat{v},\hat{\omega})^T$ from the motion sensors, we obtain the prediction of the state $\hat{\boldsymbol{x}}_{k+1}$

$$\begin{aligned} \hat{\boldsymbol{x}}_{k+1} &= (\hat{x}_{k+1},\hat{y}_{k+1},\hat{\theta}_{k+1},\hat{p}_{k+1},\hat{q}_{k+1},\hat{r}_{k+1})^T \\ &= \boldsymbol{f}(\hat{\boldsymbol{x}},\hat{\boldsymbol{m}}) \\ &= \boldsymbol{f}(\hat{x}_k,\hat{y}_k,\hat{\theta}_k,\hat{p}_k,\hat{q}_k,\hat{r}_k,\hat{v}_k,\hat{\omega}_k) \end{aligned} \tag{10}$$

and

$$\begin{aligned} \boldsymbol{f}(\boldsymbol{x},\boldsymbol{m}) &= \boldsymbol{f}(x,y,\theta,p,q,r,v,\omega) \\ &= \begin{bmatrix} x+\{v/(1+p)\}\Delta t\cos\theta \\ y+\{v/(1+p)\}\Delta t\sin\theta \\ \theta+\{(\omega-r)/(1+q)\}\Delta t \\ p \\ q \\ r \end{bmatrix} \end{aligned} \tag{11}$$

Next we will derive the update equation of the covariance matrix. Let $\boldsymbol{x}$ and $\boldsymbol{m}$ be true state and motion, and denote them.

$$\begin{aligned} \hat{\boldsymbol{x}} &= \boldsymbol{x}+\Delta\boldsymbol{x} \\ \hat{\boldsymbol{m}} &= \boldsymbol{m}+\Delta\boldsymbol{m} \end{aligned} \tag{12}$$

$\Delta\boldsymbol{x}$ and $\Delta\boldsymbol{m}$ are the errors included in $\hat{\boldsymbol{x}}$ and $\hat{\boldsymbol{m}}$, and they are assumed to be Gaussian and uncorrelated. By putting (12) into (10),

$$\begin{aligned} \hat{\boldsymbol{x}}_{k+1} &= \boldsymbol{f}(\boldsymbol{x}_k+\Delta\boldsymbol{x}_k,\boldsymbol{m}_k+\Delta\boldsymbol{m}_k) \\ &\simeq \boldsymbol{f}(\boldsymbol{x}_k,\boldsymbol{m}_k)+\left.\frac{\partial\boldsymbol{f}}{\partial\boldsymbol{x}}\right|_k\Delta\boldsymbol{x}_k+\left.\frac{\partial\boldsymbol{f}}{\partial\boldsymbol{m}}\right|_k\Delta\boldsymbol{m}_k \end{aligned} \tag{13}$$

Here, $\boldsymbol{x}_{k+1}=\boldsymbol{f}(\boldsymbol{x}_k,\boldsymbol{m}_k)$ is the true state of $\hat{\boldsymbol{x}}_{k+1}$, then the covariance matrix P_{k+1} of the state is:

$$\begin{aligned} P_{k+1} &= E[\Delta\boldsymbol{x}_{k+1}^T\Delta\boldsymbol{x}_{k+1}] \\ &= E[(\hat{\boldsymbol{x}}_{k+1}-\boldsymbol{x}_{k+1})^T(\hat{\boldsymbol{x}}_{k+1}-\boldsymbol{x}_{k+1})] \end{aligned} \tag{14}$$

where $E[\cdot]$ is the expectation operator.

From the above two equations (13), (14), we obtain

$$\begin{aligned} P_{k+1} &= \left.\frac{\partial\boldsymbol{f}}{\partial\boldsymbol{x}}\right|_k P_k\left.\frac{\partial\boldsymbol{f}}{\partial\boldsymbol{x}}\right|_k^T+\left.\frac{\partial\boldsymbol{f}}{\partial\boldsymbol{m}}\right|_k M\left.\frac{\partial\boldsymbol{f}}{\partial\boldsymbol{m}}\right|_k^T \\ &= F_xP_kF_x^T+F_mMF_m^T \end{aligned} \tag{15}$$

where, F_k and F_m are the Jacobian matrix of $\boldsymbol{f}(\boldsymbol{x},\boldsymbol{m})$ derived by $\boldsymbol{x}$ and $\boldsymbol{m}$ at time t_k respectively. This is the update equation of the covariance matrix.

The covariance matrix of the state at time t_k is $P_k=E[\Delta\boldsymbol{x}_k^T\Delta\boldsymbol{x}_k]$. The covariance matrix M of the inputs is constant and triangular because we assume they are uncorrelated.

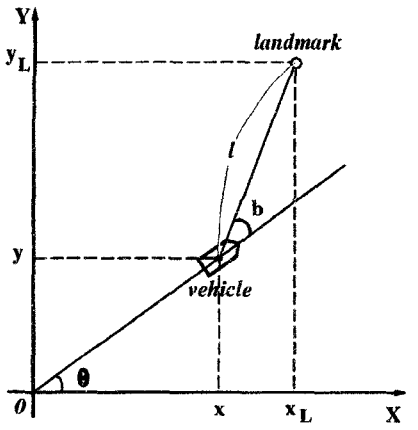

Figure 3: Vehicle and Landmark Position

4.4 Position Estimation with Landmark Detection

While no landmarks are found, only the predicted vehicle state and its covariance are calculated. When the radar detects landmarks, the vehicle state $\boldsymbol{x}$ can be estimated more precisely.

The radar sensor is fixed on top of the vehicle and pointed forwards. Consider that the vehicle detects a landmark where the vehicle state $\boldsymbol{x} = (x, y, \theta, p, q, r)$ and the landmark position (x_L, y_L). The radar outputs range l and bearing angle b. Let us denote them as a vector $\boldsymbol{l} = (l, b)$.

From Figure 3, we easily obtain

$$\begin{aligned} \boldsymbol{z} &= \begin{bmatrix} z_1(\boldsymbol{l}, \boldsymbol{x}, x_L, y_L) \\ z_2(\boldsymbol{l}, \boldsymbol{x}, x_L, y_L) \end{bmatrix} \\ &= \begin{bmatrix} \{x - x_L + r\cos(\theta + b)\}^2 \\ \{y - y_L + r\sin(\theta + b)\}^2 \end{bmatrix} = 0 \end{aligned} \quad (16)$$

Only the predicted vehicle position and orientation $\boldsymbol{x}$ are obtained which contain error $\Delta\boldsymbol{x}$, then

$$\boldsymbol{x} = \hat{\boldsymbol{x}} + \Delta\boldsymbol{x} \quad (17)$$

Given radar output $\hat{\boldsymbol{l}}$ with error $\Delta\boldsymbol{l}$, then

$$\boldsymbol{l} = \hat{\boldsymbol{l}} + \Delta\boldsymbol{l} \quad (18)$$

Putting (17), (18) into (16) and linearizing equation (16) with the first order derivatives of $\boldsymbol{x}$ and $\boldsymbol{l}$, we obtain

$$\begin{aligned} \boldsymbol{z} \simeq & \begin{bmatrix} z_1(\hat{\boldsymbol{l}}, \hat{\boldsymbol{x}}, x_L, y_L) \\ z_2(\hat{\boldsymbol{l}}, \hat{\boldsymbol{x}}, x_L, y_L) \end{bmatrix} + \begin{bmatrix} \frac{\partial z_1}{\partial \boldsymbol{x}}\Big|_* \\ \frac{\partial z_2}{\partial \boldsymbol{x}}\Big|_* \end{bmatrix} \Delta\boldsymbol{x} \\ & + \begin{bmatrix} \frac{\partial z_1}{\partial \boldsymbol{l}}\Big|_* \\ \frac{\partial z_2}{\partial \boldsymbol{l}}\Big|_* \end{bmatrix} \Delta\boldsymbol{l} = 0 \end{aligned} \quad (19)$$

$$\hat{\boldsymbol{z}} - H\Delta\boldsymbol{x} - \Delta\boldsymbol{z} = 0 \quad (20)$$

or

$$\hat{\boldsymbol{z}} = H\Delta\boldsymbol{x} + \Delta\boldsymbol{z} \quad (21)$$

where

$$\begin{aligned} \hat{\boldsymbol{z}} &= \begin{bmatrix} z_1(\hat{\boldsymbol{l}}, \hat{\boldsymbol{x}}, x_L, y_L) \\ z_2(\hat{\boldsymbol{l}}, \hat{\boldsymbol{x}}, x_L, y_L) \end{bmatrix} \\ H &= Z_x = \begin{bmatrix} -\frac{\partial z_1}{\partial \boldsymbol{x}}\Big|_* \\ -\frac{\partial z_2}{\partial \boldsymbol{x}}\Big|_* \end{bmatrix} \\ \Delta\boldsymbol{z} &= Z_l\Delta\boldsymbol{l}, \quad Z_l = \begin{bmatrix} -\frac{\partial z_1}{\partial \boldsymbol{l}}\Big|_* \\ -\frac{\partial z_2}{\partial \boldsymbol{l}}\Big|_* \end{bmatrix} \Delta\boldsymbol{l} \end{aligned} \quad (22)$$

$*$ denotes at the point $\boldsymbol{x} = \hat{\boldsymbol{x}}, \boldsymbol{l} = \hat{\boldsymbol{l}}$

Equation(21) describes error in the measurement process. $\hat{\boldsymbol{z}}$ is the observation obtained by the radar measurement with known $\hat{\boldsymbol{x}}$ and (x_L, y_L), and H is the observation matrix which is multiplied not by the vehicle state directly but by the state error $\Delta\boldsymbol{x}$. $\Delta\boldsymbol{z}$ represents errors (noise) in the observation.

Now we are almost ready to derive the equations of position estimation.

Let R be a covariance matrix of Δz.

$$\begin{aligned} R &= E[\Delta\boldsymbol{z}^T\Delta\boldsymbol{z}] \\ &= Z_l^T E[\Delta\boldsymbol{l}^T\Delta\boldsymbol{l}]Z_l \\ &= Z_l^T \begin{bmatrix} \sigma_l^2 & 0 \\ 0 & \sigma_b^2 \end{bmatrix} Z_l \end{aligned} \quad (23)$$

where we assume that the errors of the radar measurements l and b are Gaussian and uncorrelated, with variances σ_l^2 and σ_b^2 respectively. Consider that the observation occurred at time t_k and put suffix k in every time dependent variable such as $H_k, R_k, \hat{\boldsymbol{z}}_k$. And let $\boldsymbol{x}_k(-)$ and $P_k(-)$ denote the predicted state and covariance matrix at t_k. With the theory of the Kalman filter, we get equations of estimated position $\boldsymbol{x}_k(+)$ and covariance matrix $P_k(+)$ as follows.

$$\begin{aligned} \boldsymbol{x}_k(+) &= \boldsymbol{x}_k(-) + P_k(+)H^T R^{-1}\hat{\boldsymbol{z}}_k \\ P_k(+) &= [P_k(-)^{-1} + H_k^T R^{-1} H]^{-1} \end{aligned} \quad (24)$$

5 Map Building and Navigation

5.1 Map Building without Previous Knowledge of Landmarks

The map we intend to build consists of roadways and landmarks. A roadway is a path to be followed, and is represented as series of points on the center of the road. Landmark information consists of position and other attributes such as type and sensor dependent characteristics.

Initially we have no knowledge about the road and landmarks. We want to build a map by running the vehicle manually and measuring vehicle motion and radar observations.

Errors in predicted position and orientation accumulate while no landmark is detected. The errors have to be corrected by position estimation with landmarks.

During a single run, when an object is first detected its position is noted. If an object is detected in the same place again, such as in the next radar measurement, then it is assumed to be the same object observed before and the object is labelled as a landmark. Any errors in motion estimation since the first detection of this landmark will show up as errors in vehicle position. The subsequent sightings of the landmark are used to improve the vehicle position estimate, and to decrease the effect of motion errors.

5.2 Elimination of Radar Noises

Landmarks are reflectors (usually corner cubes) that we installed or naturally existing objects (usually metallic objects) which reflect millimeter wave radar strongly. However the radar detects not only landmarks, but also any objects that reflect the wave. Some of those objects may not be desirable as landmarks and should be treated as noise.

Elimination of radar noise is not easy. We do not try to distinguish noise, but statistically reduce the effect of the noise: first, objects measured only once at the same place are recorded in a map, but are not labelled as landmarks. Second we introduce the ambiguity of a landmark's position represented by variance σ_{xL}^2 and σ_{yL}^2. These variances are set to be large, so observation of the landmark has a relatively small effect on vehicle position estimation. A sufficient number of observations will lead to a correct position estimation, while a few noisy observations will have little effect.

To introduce the variance of landmark position, merge (x_L, y_L) into l in equation (19) and (22), then we get

$$R = Z_l^T \begin{bmatrix} \sigma_l^2 & 0 & 0 & 0 \\ 0 & \sigma_b^2 & 0 & 0 \\ 0 & 0 & \sigma_{xL}^2 & 0 \\ 0 & 0 & 0 & \sigma_{yL}^2 \end{bmatrix} Z_l \quad (25)$$

This R will be used in position estimation instead of equation (23).

5.3 Errors in Landmark Position

The accuracy of the radar is usually high. The error is typically less than 0.1m in range and less than 0.1 degree in bearing angle.

The radar measurement is combined with the position of the vehicle to calculate the position of detected objects, then errors in objects position are the sum of errors in radar measurement and vehicle position. However our experiment shows that the dispersion of object positions is larger than expected. The cause of these errors could be multi-path dusturbance caused by nearby objects or timing problem of the radar process and the positioning process running in parallel; we are currently working to diagnose and reduce these errors. Figure 4 and 5 shows measured positions of several objects when the vehicle ran along the x-axis. The upper left cluster in Figure 4 is a corner cube. Other objects in the both figures are a small number of naturally existing objects beside the road. Especially in Figure 5, the plotted positions spread over 10m×2m square and are not distinguishable as a few objects.

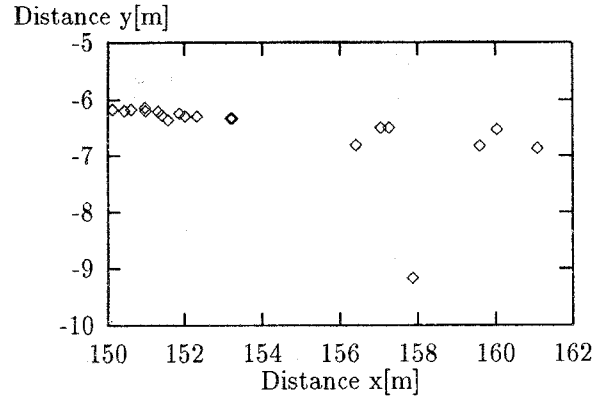

Figure 4: Detected landmark distribution

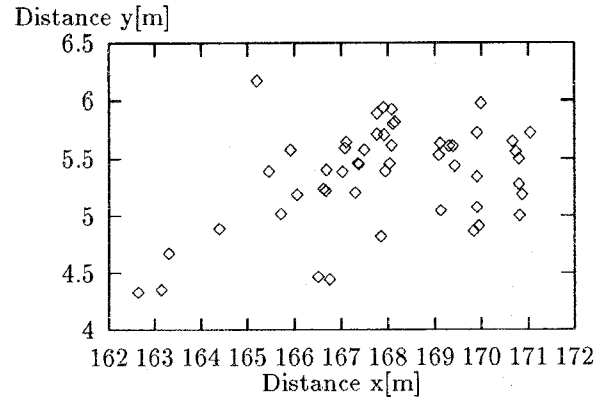

Figure 5: Detected landmark distribution

From these results, we have to assume a relatively large variance in measured landmark positions.

5.4 Experimental Results

Map Building. Corner cubes are placed every fifty meters along the road to be used as landmarks. In addition several metaric objects exist along the road such as light poles and traffic signs and these objects are also used as landmarks.

Raw dead reckoning trajectories of the vehicle driven by a human are shown in Figure 6. The vehicle started from the origin in the figure and moved at 50km/h. Each trajectory differs and contains accumulated er-

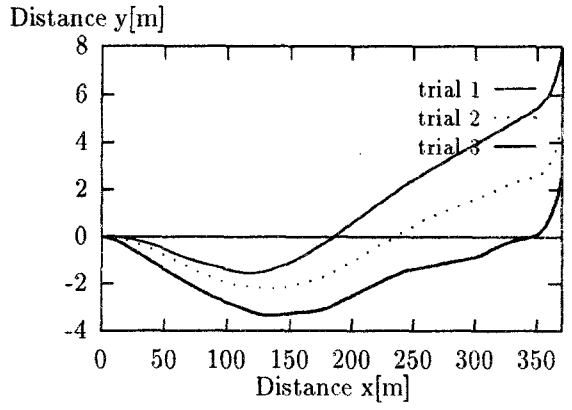

Figure 6: Vehicle trajectories by dead reckoning

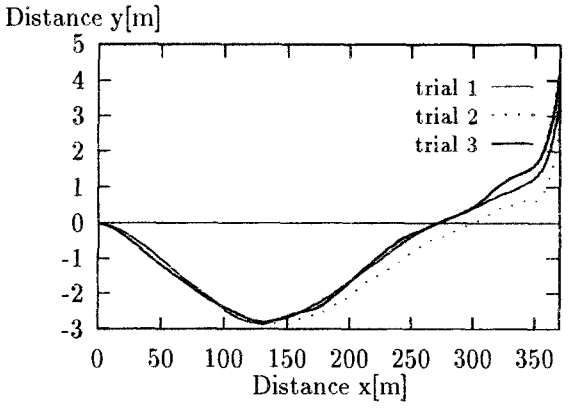

Figure 7: Vehicle trajectories corrected by landmark detection and position estimation

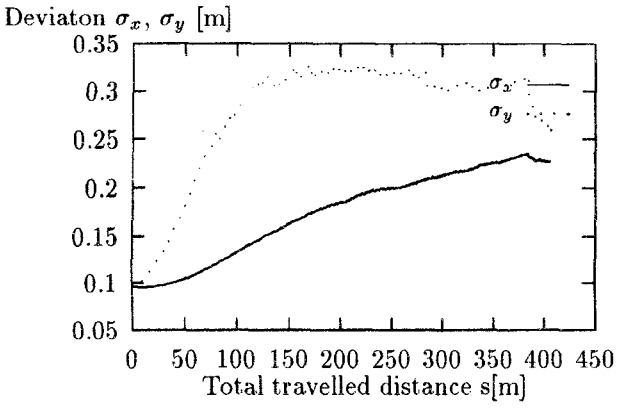

Figure 8: Estimated errors in vehicle position while map building - σ_x, σ_y

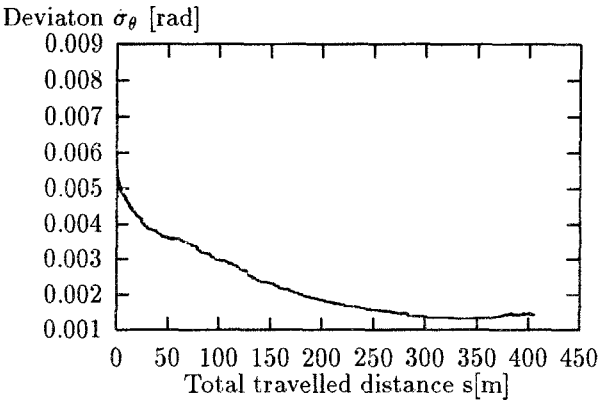

Figure 9: Estimated errors in vehicle orientation while map building - σ_θ

rors in motion sensing. The raw trajectories cannot be used as a map.

Trajectories corrected by using landmarks are shown in Figure 7. The method described in 5.1 is used without previous knowledge of landmarks. The trajectories are closer than raw dead reckoning. Figures 8 and 9 show the estimated standard deviation of errors in vehicle position and orientation of trial 1 in Figure 7. The rapid error growth seen in raw dead reckoning is suppressed, and the estimated error in the vehicle orientation, which is very important in position estimation, is decreasing. This means the built map is accurate; errors in the map do not diverge and are kept under certain values.

Navigation with Map. The map built without previous knowledge of landmarks can be effectively used for navigation. We would like to show that the vehicle can estimate its position and orientation with the built map.

Figure 10 shows a path and landmarks in the map and trajectories (series of estimated position) when the vehicle was driven by a human along the road. The trajectories of both trials are estimated well and very close to the original path in the map. The differences are within the expected human driving errors on the same path.

Estimated errors of vehicle position are suppressed and kept under certain values as shown in Figure 11 and 12.

6 Conclusion

For position based navigation of Automated Highway System, a method of map building without previous knowledge of landmarks was proposed and verified by experiments. The system with radar and motion sensors was introduced, and the extended Kalman filter was designed for position estimation. The model of the filter includes sensing errors of motion sen-

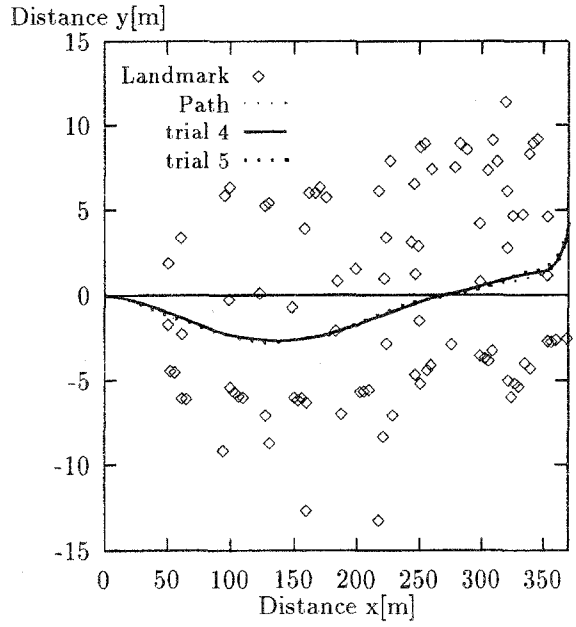

Figure 10: Navigated vehicle trajectories

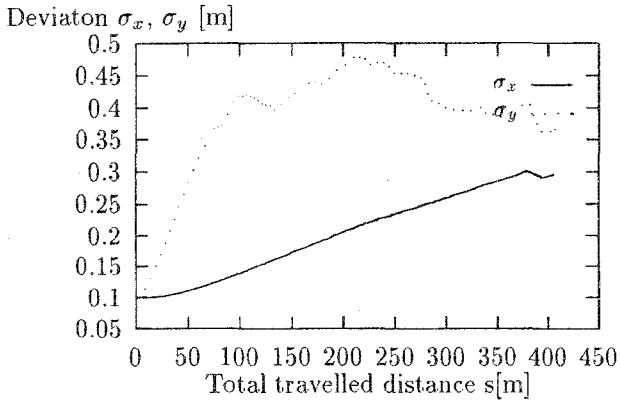

Figure 11: Estimated errors in vehicle position while navigation - σ_x, σ_y

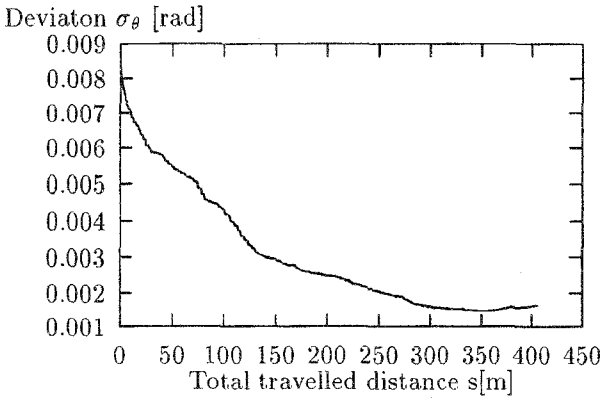

Figure 12: Estimated errors in vehicle orientation while navigation - σ_θ

sors and landmark measurement by the radar sensor. The experiments showed that a map can be built without previous knowledge of landmarks, and after the map building vehicle position was estimated accurately while the vehicle moved along the path in the map.

In our ongoing work, we are reducing the errors in radar sensing, and therefore in landmark positions. We are also preparing for autonomous driving. While the experiments shown here demonstrate that vehicle position can be accurately obtained for a human driver, it is our goal to have the vehicle positions obtained accurately enough for fully automated driving, based solely on position estimation. The next step after that is to integrate position-based driving with vision-based road following, and to measure the accuracy and reliability of the combined system.

Aknowledgement. : This research has been supported by USDOT under Cooperative Agreement Number DTFH61-94-X-00001 as part of the National Automated Highway System Consortium.

References

[1] Dean A. Pomerleau "Neural Network Perception for Mobile Robot Guidance" Kluwer Academic Publishers, 1993

[2] Dean A. Pomerleau "RALPH: Rapidly Adapting Lateral Position Handler" IEEE Symposium on Intelligent vehicle, September 1995

[3] Volker Graefe and Klaus Dieter Kuhnert "Vision-based Autonomous Road Vehicles" in Vision-based Vehicle Guidance, pp.1-29 Springer-Verlag 1992

[4] Hugh F.Durrant-Whyte "An Autonomous Guided Vehicle for Cargo Handling Application" The International Journal of Robotics Research Vol.15 No.5 October 1996, pp.407-440

[5] Katsumi Kimoto and Shin'ichi Yuta "Sonar Based Outdoor Navigation – Navigation using Natural Landmarks –", Proc. of International Conference on Advanced Robots, Nov. 1993, pp239-244

[6] Dirk Langer "Proposal for an Integrated MMW Radar System for Outdoor Navigation" Technical Report, CMU-RI-TR-96-15, 1996 Carnegie Mellon University

[7] N.Currie and C.Brown "Principles and Application of Millimeter-wave Radar" Artec House, 1987